Supporting Information

Diaz-Rohrer et al. 10.1073/pnas.1404582111

SI Materials and Methods

Cell Culture and Transfection. Rat basophilic leukemia (RBL) cells were cultured in medium containing 60% Eagle's Minimum Essential Medium (MEM), 30% RPMI, 10% FCS, 2 mM glutamine, 100 U/mL penicillin, and 100 μg/mL streptomycin at 37 °C in humidified 5% CO_2. Transfection was done by nucleofection (Amaxa) using the protocols provided with the reagents. Four to six hours after transfection, cells were washed with PBS and then were incubated with serum-free medium overnight. To synchronize the cells, 1 h before preparation of giant plasma membrane vesicles (GPMV), the cells were given full-serum medium. For inhibition of glycosphingolipid synthesis, cells were treated with *N*-nonyl-deoxygalactonojirimycin (C9DGJ) for 48 h in full medium. Brefeldin A (BFA) and bafilomycin A1 (Cayman Chemicals) were used at 100 μg/mL and 50 μM, respectively, for at least 2 h. For inhibition of dynamin-mediated endocytosis, Dynasore (Sigma) was used up to 100 μM with no effect on trLAT trafficking. For stable expression, transfected cells were selected in 0.2 mg/mL G418.

Constructs and Generation of Mutants. The transmembrane domain (TMD) of linker for activation of T-cells (trLAT), its palmitoylation mutants, and transferrin receptor (TfR)-GFP have been described (1). The amino acid sequence of WT trLAT is MEEAILVPCVLGLLLLPILAMLMALCVHCHRLPGS followed by a short linker (GS) and monomeric RFP (mRFP). TMD mutants were generated by synthetic production (Genscript) of the gene of interest and subsequent cloning of the mutant sequence into the trLAT construct. Mutant identities were confirmed by sequencing. TMD length was defined as the number of amino acids between the two charged residues flanking the hydrophobic stretch (E3 and H28). All constructs were designed with the same upstream and downstream elements and were driven by the same promoter and thus were expected to have consistent expression. We verified similar expression of trLAT-WT, trLAT missing six amino acids from the hydrophobic core (trLAT-Δ6core), and trLAT with all TMD amino acids (except the palmitoylation sites) mutated to leucines (trLAT-allL) by Western blotting (Fig. S7*A*).

mrLAT is a minimal raft-partitioning construct containing only the transmembrane (TM) and flanking residues of LAT, generated by commercial gene synthesis, with the sequence MEAILVPCVLGLLLLPILAMLMALCVHCH, then linker, then mRFP.

Non-LAT constructs were generated by commercial gene synthesis and designed to contain the TMD and juxtamembrane amino acids of CD4 (V393-C418), LIME (M1-A37), and PAG/Cbp (M1-P46) or versions of those constructs missing six amino acids from the either the hydrophobic core (Δ6core) or the exoplasmic face of the TMD (Δ6exo). The sequences are

trCD4: MEEVQPMALIVLGGVAGLLLFIGLGIFFCVHCHR

trCD4_Δ6exo: MEEVQPM_____GVAGLLLFIGLGIFFCVHCHR

trCD4_Δ6core: MEEVQPMALIVLGGVAGL_____GIFFCVHCHR

trLIME: MGLPVSWAPPALWVLGCCALLLSLWALCTACRRPEDA

trLIME_Δ6exo: MGLPVSWAP_____GCCALLLSLWALCTACRRPEDA

trLIME_Δ6core: MGLPVSWAPPALWVL_____LSLWALCTACRRPEDA

trPAG: MGPAGSLLGSGQMQITLWGSLAAVAIFFVITFLIFLCSSCDREKKP

trPAG_Δ6exo: MGPAGSLLGSGQMQITLW_____AIFFVITFLIFLCSSCDREKKP

trPAG_Δ6core: MGPAGSLLGSGQMQITLWGSLAAV_____TFLIFLCSSCDREKKP

which are followed by the same linker and mRFP as trLAT.

GPMV Isolation and Partitioning Measurements. Before GPMV isolation, cell membranes were stained with 5 μg/mL of FAST-DiO (Invitrogen), a green fluorescent lipidic dye that strongly partitions to disordered phases because of double bonds in its fatty anchors (2). GPMVs were isolated and imaged as described (3, 4). The trends for partitioning of trLAT constructs were independent of the isolation procedure, with *N*-ethyl maleimide (NEM) and paraformaldehyde (PFA)/DTT isolations yielding similar observations (Figs. 1 and 2). Moreover, neither localization (Fig. 8*A*) nor partitioning (Fig. 8*B*) was cell-type dependent, with both NIH 3T3 fibroblasts and HEK cells showing results similar to those seen with RBLs.

Cell Labeling and Immunofluorescence. Before plasma membrane (PM) labeling, transfected RBL cells were incubated for 1 h in full medium containing 40 μg/mL cycloheximide to stop protein translation. This treatment was designed to clear the biosynthetic organelles of newly synthesized proteins and thereby reveal the steady-state distribution of the trLAT mutants; consistent with this design, neither PM or Golgi staining was observed for trLAT-WT (Fig. S3*A*). For PM labeling, surface-exposed proteins were nonspecifically biotinylated as described (1), fixed with 4% paraformaldehyde, then stained with 10 μg/mL fluorescein-streptavidin (Vector Laboratories), or Texas Red-streptavidin for TfR-GFP experiments.

For immunofluorescence labeling of late endosomes, an anti-LPBA mouse monoclonal antibody was used (a kind gift of Jean Grünberg, University of Geneva, Geneva). For labeling of lysosomes, an antibody against the lysosomal marker LAMP1 (H4A3; Santa Cruz Biotechnology), LysoTracker (Invitrogen), and incubation with 0.1 mg/mL 50 kDa dextran (coupled to Alexa 488) (Invitrogen) gave identical results. For immunolabeling of early endosomes (EEs), we used anti-Rab5 (Rb polyclonal 3457; Sigma). Fluorescent secondaries were purchased from Invitrogen.

Imaging and Image Processing. Imaging was performed on a confocal microscope (Zeiss LSM510; 63× oil immersion) using the appropriate filter sets for GFP/RFP fluorescence. Three confocal slices were quantified for each cell, and at least 15 cells per mutant were measured. Image processing was done by a fully automated, custom image-processing protocol in Fiji. This protocol yielded %PM values that were in agreement with visual predictions, although there was some overestimation of surface localization for mutants with peripheral, but not PM, staining (e.g., Fig. S3*H*).

Acyl–Biotinyl Exchange to Analyze Whole-Membrane and PM Palmitoylation. For analysis of PM palmitoylation of trLAT mutants, we prepared PM-only fractions by the GPMV protocol. Briefly, GPMV were gathered as described (3) from two 10-cm

dishes of 80% confluent RBLs stably transfected with trLAT constructs and then were pelleted for 1 h at 20,000 × *g* to yield the PM-only fraction. This fraction was highly enriched in a PM marker (endogenous LAT) and depleted of calnexin, a marker of the endoplasmic reticulum (ER), the most abundant non-plasmalemmal membrane (Fig. S7*B*). The relative enrichment of PM compared with ER was 250× in GPMVs relative to whole cells.

Palmitoylation analysis was done using acyl–biotinyl exchange (ABE) as described (5). Briefly, membranes were lysed in 2% SDS-containing buffer, and free cysteines were blocked by 10 mM NEM. Then, palmitoylated cysteines were liberated by 0.4 M hydroxylamine and labeled with biotin-HPDP (Pierce). Biotinylated proteins were pulled down using streptavidin-agarose and eluted with 1% 2-mercaptoethanol. Chloroform/methanol precipitations were performed twice between each step to remove chemicals. After elution, 25 uL out of 100 uL of the final eluate was run as the palmitoylated fraction, compared with 3 uL out of 100 uL of the input fraction. For quantification, densitometry of scanned films was done by ImageJ, and the palmitoylated signal was divided by the input; then this ratio was normalized to the same ratio for endogenous LAT, yielding a preparation-independent relative palmitoylation level for each trLAT construct. For palmitoylation analysis of trLAT-allL (Fig. S4*B*), cells were pretreated with BFA to prevent lysosomal degradation.

1. Levental I, Lingwood D, Grzybek M, Coskun U, Simons K (2010) Palmitoylation regulates raft affinity for the majority of integral raft proteins. *Proc Natl Acad Sci USA* 107(51):22050–22054.
2. Levental I, Grzybek M, Simons K (2011) Raft domains of variable properties and compositions in plasma membrane vesicles. *Proc Natl Acad Sci USA* 108(28): 11411–11416.
3. Sezgin E, et al. (2012) Elucidating membrane structure and protein behavior using giant plasma membrane vesicles. *Nat Protoc* 7(6):1042–1051.
4. Levental I, et al. (2009) Cholesterol-dependent phase separation in cell-derived giant plasma-membrane vesicles. *Biochem J* 424(2):163–167.
5. Wan J, Roth AF, Bailey AO, Davis NG (2007) Palmitoylated proteins: purification and identification. *Nat Protoc* 2(7):1573–1584.

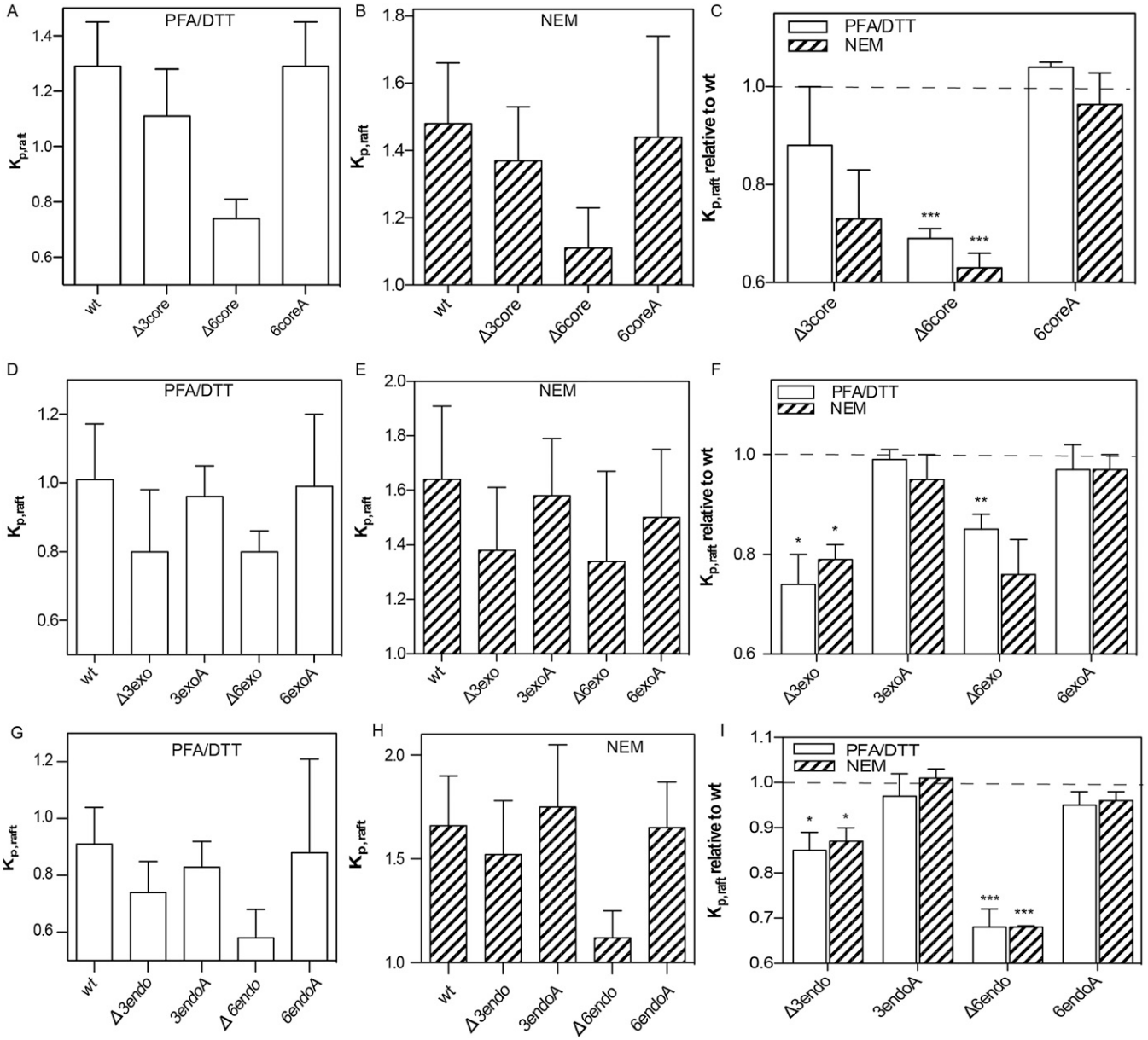

Fig. S1. Raf-phase partitioning is a function of TMD length. The raft-phase partition coefficient ($K_{p,raft}$) of trLAT mutated in amino acids of the hydrophobic core (*A*–*C*), exoplasmic (*D*–*F*), or endoplasmic (*G*–*I*) parts of the TMD. Shown are representative datasets of $K_{p,raft}$ in PFA/DTT (*A*, *D*, *G*) and NEM (*B*, *E*, *H*) GPMVs. Data shown are average ± SD from 10–15 vesicles per experiment. Data shown in *C*, *F*, and *I* are average ± SEM from three to six independent experiments (*$P < 0.05$; **$P < 0.01$; ***$P < 0.001$).

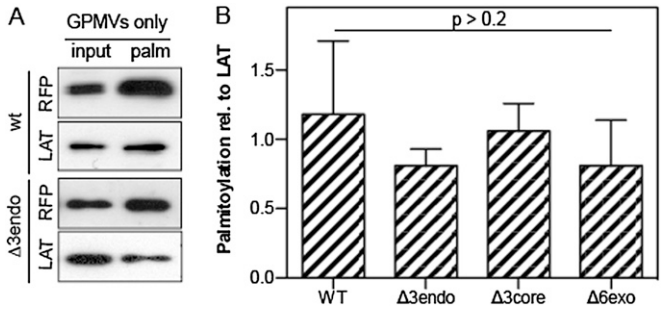

Fig. S2. Palmitoylation of trLAT constructs at the PM. (*A*) Representative Western blots of palmitoylation measured by ABE for GPMV preparations of cells transfected with trLAT constructs demonstrate that the palmitoylation level at the PM is similar for the WT and a truncation construct. (*B*) Relative palmitoylation was quantified by normalizing the palmitoylation (palm)/input ratio for each construct relative to endogenous LAT. Palmitoylation of trLAT-WT was indistinguishable from endogenous LAT. None of the TMD truncations tested were statistically different from the WT in these preparations. (Data are shown as the average ± SD from three to five independent experiments per construct).

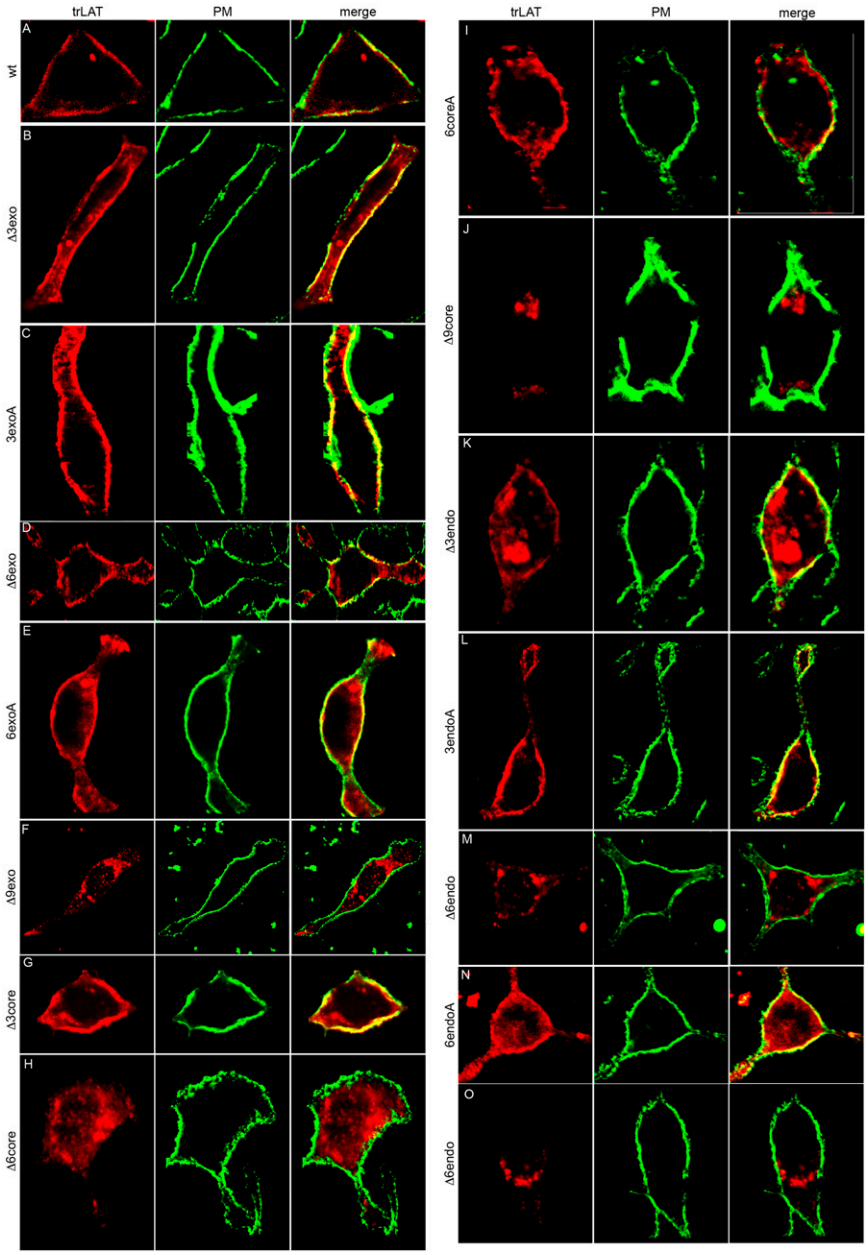

Fig. S3. Subcellular distribution of trLAT mutants. Images of the various trLAT TMD mutants (red; for sequences see Table S1) with the biotinylated PM counterstained with fluorescein-streptavidin (green). Mutants with normal TMD lengths tended to localize at the PM, whereas deletion mutants with shorter TMDs are in the membranes of intracellular organelles, usually late endosomes (Fig. 3*D*) and lysosomes (Fig. 3*E*). Some substitution mutants with normal TMD length showed slightly aberrant localization; for example, trLAT with all TMD amino acids (except the palmitoylation sites) mutated to alanines (6coreA) (*I*) was enriched at the PM but also had significant intracellular localization.

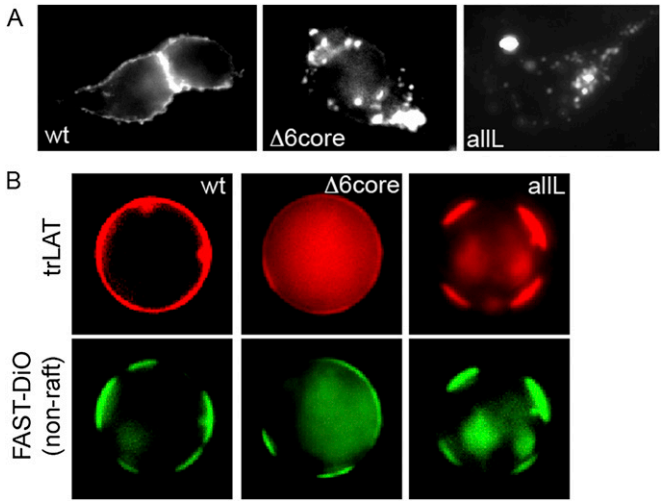

Fig. S4. Partitioning and localization are not cell-type dependent. (*A*) Epifluorescence micrographs of trLAT constructs expressed in NIH 3T3 fibroblasts demonstrate that trLAT-WT is localized to the PM, whereas -allL and -Δ6core are in intracellular late endosomes, mirroring their distribution in RBLs (Figs. 3 and 4). (*B*) GPMVs derived from NIH 3T3 cells transfected with trLAT mutants and prestained with the nonraft marker FAST-DiO demonstrate that raft partitioning of these constructs in vesicles derived from these cells is identical to that in vesicles derived from RBLs (Figs. 2 and 4); i.e., trLAT-WT is distributed approximately equally between the raft and nonraft phases, -allL is completely excluded from the raft phase, and -Δ6core is somewhat raft depleted.

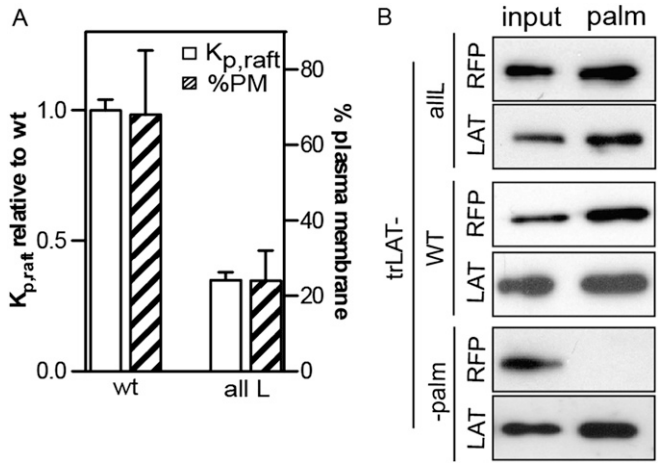

Fig. S5. Partitioning, localization, and palmitoylation of trLAT-allL. (*A*) Quantification of PM localization and $K_{p,raft}$ for the trLAT-allL variant show that both are dramatically reduced compared with trLAT-WT. (*B*) Representative Western blots showing the palmitoylation of the trLAT-allL construct and endogenous LAT as measured by ABE. trLAT-WT and -allL are efficiently palmitoylated to approximately the same level as endogenous LAT, whereas a palmitoylation-site mutant shows no detectable palmitoylation. For the ABE experiments, cells were pretreated with BFA to prevent lysosomal degradation of trLAT-allL.

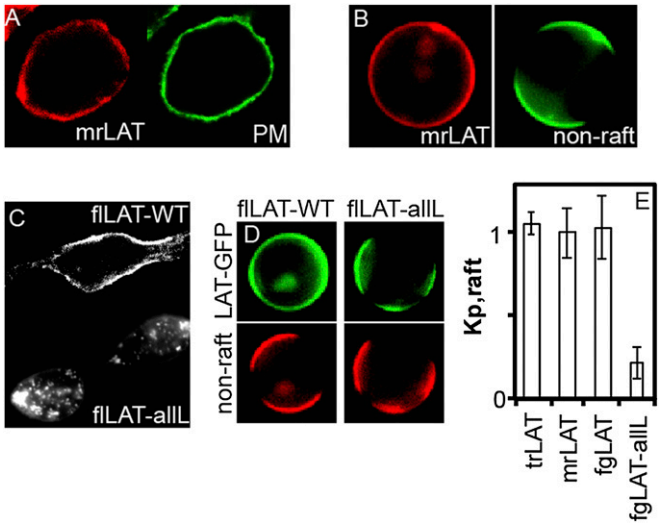

Fig. S6. Partitioning and localization of full-length and minimal LAT. (*A*) Confocal micrograph of a minimal LAT construct (mrLAT) containing only the TM residues and those required for translation and trafficking. This construct traffics efficiently to the PM. (*B*) It also partitions to the raft domain in GPMVs at parity with trLAT ($K_{p,raft}$ relative to trLAT = 1.01 ± 0.06 from three independent experiments). (*C–E*) Full-length LAT-GFP localizes to the PM, whereas a non–raft-targeting TMD (allL) inserted into the full-length protein leads to endosomal accumulation. Taken together, these results confirm that raft partitioning via the TMD is necessary and sufficient for PM localization of LAT.

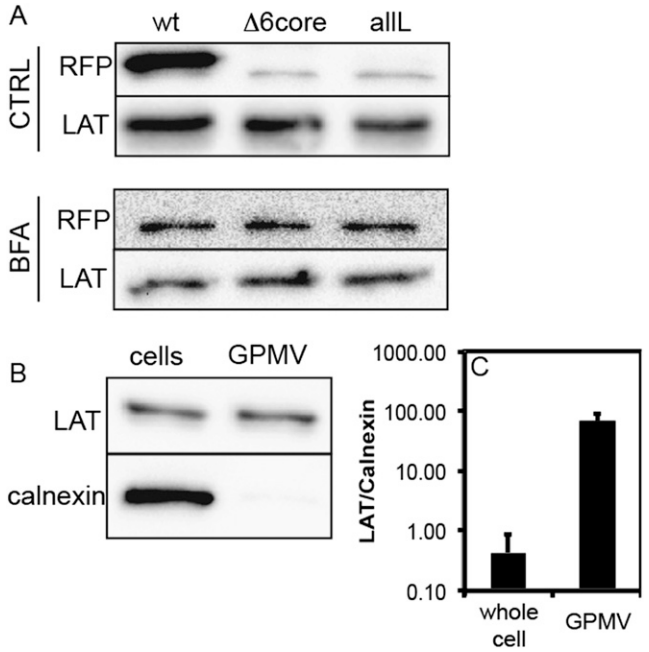

Fig. S7. BFA-sensitive degradation of nonraft LAT constructs and characterization of GPMVs as clean PM preparation. (*A*) Western blots of whole-cell lysates from RBL cells stably expressing trLAT constructs. In untreated cells, the expression of nonraft, lysosome-targeted variants (-allL and -Δ6core) was lower than that of trLAT-WT, likely because of lysosomal degradation. When endosomal trafficking was interrupted by BFA, expression of all constructs was at parity. Thus, the differences in partitioning and localization of trLAT constructs were not a function of expression level. Endogenous LAT is shown as a loading control. (*B*) Western blotting of whole-cell lysates and isolated GPMVs against a PM marker (LAT) and an ER marker (calnexin) shows that the GPMV preparation is highly enriched in the PM compared with the other most abundant cellular membrane. (*C*) Quantification (mean ± SD of three independent experiments) suggests ∼250× enrichment of PM in GPMVs.

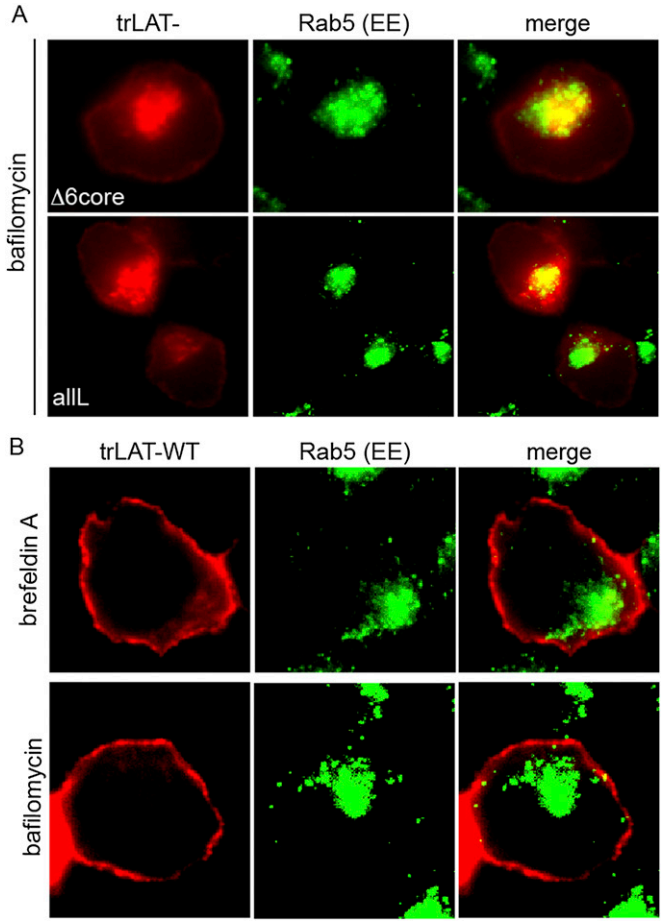

Fig. S8. Specific redistribution of nonraft trLAT construct by bafilomycin. (*A*) Bafilomycin (50 μM) induced a redistribution of both trLAT-Δ6core and trLAT-allL from lysosomes (Figs. 3 and 4) to the PM and EE. (*B*) Neither bafilomycin nor BFA had an observable effect on the PM localization of trLAT-WT.

Table S1. trLAT mutant sequences

trLAT mutant	TMD length (amino acids)	Type	Sequence
WT	24	Wild type	MEEAILVPCVLGLLLLPILAMLMALCVHC...
Δ3exo	21	Deletion	MEE___VPCVLGLLLLPILAMLMALCVHC...
3exoA	24	Substitution	MEE**AAAA**PCVLGLLLLPILAMLMALCVHC...
Δ6exo	18	Deletion	MEE_____VLGLLLLPILAMLMALCVHC...
6exoA	24	Substitution	MEEA**AAAAA**VLGLLLLPILAMLMALCVHC...
9exoA	24	Substitution	MEEA**AAAAAAAA**LLLLPILAMLMALCVHC...
Δ3core	21	Deletion	MEEAILVPCVLG___LPILAMLMALCVHC...
Δ6core	18	Deletion	MEEAILVPCVLG_____LAMLMALCVHC...
6coreA	24	Substitution	MEEAILVPCVLG**AAAAAA**LAMLMALCVHC...
Δ3endo	21	Deletion	MEEAILVPCVLGLLLLPILAML___CVHC...
3endoA	24	Substitution	MEEAILVPCVLGLLLLPILAML**AAA**CVHC...
Δ6endo	18	Deletion	MEEAILVPCVLGLLLLPIL_____CVHC...
6endoA	24	Substitution	MEEAILVPCVLGLLLLPIL**AAAAAA**CVHC...
allL	24	Composition	MEELLLLLLLLLLLLLLLLLLLLLCVHC...
C26A	24	Palmitoylation	MEEAILVPCVLGLLLLPILAMLMAL**A**VHC...
C29A	24	Palmitoylation	MEEAILVPCVLGLLLLPILAMLMALCVH**A**...

Mutants of varying TMD length and composition were generated from trLAT (1), a model TM protein containing the TMD and the juxtamembrane portion of LAT fused to mRFP. Boldface type highlights mutated amino acids.